Lay Down Simulation of Viscoelastic Fluids Using the Hybrid Immersed-Boundary Method

Andreas Mark[1], Simon Ingelsten[2] and Fredrik Edelvik[3]
Fraunhofer Chalmers Research Centre
Chalmers Science Park
SE-412 88 Göteborg

[1] *andreas.mark@fcc.chalmers.se*
[2] *simon.ingelsten@fcc.chalmers.se*
[3] *fredrik.edelvik@fcc.chalmers.se*

Abstract

Lay down of viscoelastic fluids is common in several manufacturing processes. In the automotive industry, sealing material is sprayed onto the vehicle body to prevent water leakage into cavities and to reduce noise. To predict the deposition and lower the environmental impact by reducing material consumption, a detailed physical understanding of the process is important. In this work the resulting surface multi-phase flow is modeled and simulated in IBOFlow, the in-house multi-phase flow solver at the Fraunhofer-Chalmers Centre. In the solver the two phase flow is modelled by the volume of fluid method and the viscoelastic fluid by a general Carreu rheology model. In the solver the scanned or CAD geometry is handled by the hybrid immersed boundary method and the material interface is resolved by the adaptive anisotropic octree grid. The resulting hanging octree and triangular nodes along the geometry are automatically handled by the immersed boundary method. To boost the computational performance the simulation domain is in a novel way dynamically divided into an active and an inactive part. The governing equations are only assembled and solved for in the active part, which is determined by the local position of the injection nozzle. The interface between the active and the inactive cells are handled by symmetry boundary conditions and the pressure is always set for a point inside the active domain. The sealing lay down simulation is successfully validated for a number of real sealing beads on a plate and on a Volvo V40 vehicle. Finally, the importance of resolving the nozzle in the simulation is investigated for a static case.

Keywords: immersed boundary method, sealing simulation, volume of fluid, rheology model, Carreau model

1. Introduction

Sealing material is applied to automotive bodies to cover holes and seams, where moisture otherwise might create a corrosive environment. After the vehicle bodies are coated with electro coat, the sealing material is applied by robots. In Figure 1 a number of applied sealing beads are shown.

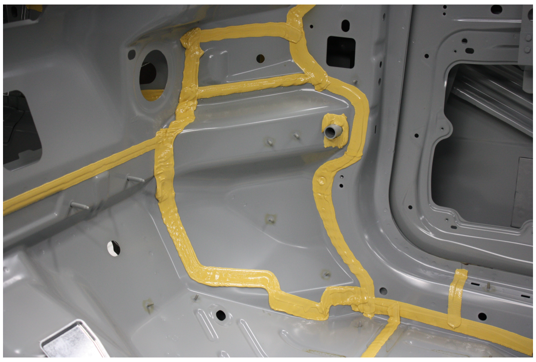

Figure 1: Flat bead sealing seams on a body-in-white.

As seen in the Figure the sealing beads are long ($\approx 1\,m$) and thin ($\approx 3\,mm$) and typically 50 meters of sealing material is applied on a vehicle body. Further, the beads overlap and penetrates into cavities and are applied in regions with complex geometry. Hence, the application sets high demand on separation of scales and the geometry handling. Further, the applied sealing material is shear thinning, that is the viscosity decays with increasing shear or force. Hence, a standard Newtonian viscosity model is not sufficient and a more complex rheology model is required. Up until now the automotive industry has relied on individual experience and physical validation for improving the complex sealing process.

However, with the increase in computational power modeling and simulation are integrated into the development of many other complex processes [3, 10]. By using simulations the risk and unforeseen cost is reduced, and further optimization is performed in the virtual prototyping stage. With virtual optimization the environmental impact and the lead time to develop new models are reduced. Further, automatic path planning of robot motions can reduce the cycle time or the number or required robots.

Not many researchers have tried to simulate the complex sealing process. In 2004 Domnick and Schneider [5] simulated the process with the commercial software Fluent. In their work the sealing material is modeled with the volume of fluid (VoF) module and a shear thinning rheology model is employed. With this approach the simulation times are very long, a boundary conforming grid is required and the import of robot paths is not streamlined. In 2011 Runqvist et al. [12] used smooth particle hydrodynamics (SPH) to simulate the sealing process. The Lagrangian framework only considers one phase (the sealing material) and due to the high impact velocity the adaptive time step is very low. However, the framework accurately captured the sealing lay down with a hollow cone applicator.

In this work, the in-house multi-phase flow solver IPS

IBOFlow [2] is employed to simulate the sealing process. The incompressible Navier-Stokes equations are discretized on an adaptive octree grid and the presence of all objects is handled by the hybrid immersed boundary method [7, 8]. Hence, moving objects are handled with minimum overhead and the mesh generation is automatic. The software also includes a very robust, novel VoF module, where the moving interface is dynamically refined. To speed up the simulations the simulation domain is in a novel way dynamically divided into an active and an inactive part.

IPS IBOFlow is integrated in the math-based software for virtual product and production realization, IPS [1]. In the IPS Virtual Paint Sealing software a detailed process simulation can be combined with sequence optimisation and motion planning to select one solution for each seam and connect them by efficient motions that minimise the cycle time. The structure of the rest of the paper is as follows: First the flow solver and rheology model are described. Then the sealing simulation framework is summarized. In the result section, the sealing lay down simulation is validated for a number of beads on a plate and on a Volvo V40 vehicle. To verify the approximate injection model, the results are compared to a resolved nozzle simulation for a static case. Finally the paper is summarized and conclusions are drawn.

2. Flow solver

An incompressible fluid is modeled by the Navier-Stokes equations,

$$\nabla \cdot \vec{u} = 0\,, \tag{1}$$

$$\rho_f \frac{\partial \vec{u}}{\partial t} + \rho_f \vec{u} \cdot \nabla \vec{u} = -\nabla p + \mu \nabla^2 \vec{u} + \vec{s}\,, \tag{2}$$

where $\vec{u}$ is the fluid velocity, ρ_f is the fluid density, p is the pressure, μ is the apparent viscosity defined as the ratio between shear stress and shear rate, $\mu = \frac{\sigma}{\dot{\gamma}}$. $\vec{s}$ is the droplet source term including the buoyancy force. The Navier-Stokes equations are discretized with the finite volume method on a dynamic Cartesian octree grid, which is automatically generated and allows adaptive grid refinements to follow moving objects. The equations are solved in a segregated way and the SIMPLEC method is used to couple the pressure and the velocity fields [6]. All variables are stored in a co-located arrangement and the pressure weighted flux interpolation is used to suppress pressure oscillations [11]. The Backward Euler scheme is used for the temporal discretization and an adaptive fluid time step is employed such that the maximum Courant number based on the fluid velocity and the movement of the applicators are restricted.

The internal boundary conditions are handled by the hybrid immersed boundary method [8]. In the method the fluid velocity is set to the local velocity of the object with an immersed boundary condition. Extrapolation and mirroring of the velocity close to the boundary are used to formulate an implicit boundary condition which is added to the operator for the momentum equations. The mirroring results in a fictitious fluid velocity field inside the immersed object. Mass conservation is ensured by excluding this velocity field in the discretized continuity equation. A thorough description of the method and an extensive validation can be found in [8].

To boost the computational performance the simulation domain is in a novel way divided into an active and an inactive part. The active part is defined by all cells laying closer than $5\,cm$ from the sealing impact positions. Further, all injection cells need to be connected with each other and cells that are not directly connected with an injection cell are made inactive (cells laying on the opposite side of a scalar surface compared to the sealing nozzle). The active region is updated every fifth time step. At every update the active cells are given local indices that are mapped to the global ones. The governing equations are only assembled and solved for the active cells but the solution is stored on the full grid. The interface between the active and the inactive cells are handled by symmetry boundary conditions and the pressure is always set for a cell inside the active domain. With this procedure the amount of active computational cells does not increase when the simulated sealing bead becomes longer. Hence, the simulation time for the first second is in the same order of magnitude as the final simulation second. Without this division the difference the would be orders of magnitudes.

The two-phase flow in the sealing application is modeled with the VoF method, where the local property of the fluid is dependent on the volume fraction. The volume fraction is transported with the local velocity field. To keep the interface between the sealing material and the air sharp a hybrid CICSAM convective scheme is adopted [13].

The apparent viscosity of the adhesive is modelled according to the Carreau model [4],

$$\mu = (\mu_0 - \mu_\infty)\left(1.0 + (\lambda\dot{\gamma})^2\right)^{0.5(N-1)} \tag{3}$$

where the apparent viscosity, μ, is dependent on the local shear rate, $\dot{\gamma}$, λ and N are material constants derived from experiments. μ_0 and $_\infty$ are the zero-shear-rate vis- cosity and the infinite-shear-rate viscosity, which represents the upper and lower Newtonian plateaus defined as

$$\lim_{\dot{\gamma}\to 0} \frac{\sigma_{xy}}{\dot{\gamma}_{xy}} = \mu_0 \quad \text{and} \quad \lim_{\dot{\gamma}\to \infty} \frac{\sigma_{xy}}{\dot{\gamma}_{xy}} = \mu_\infty. \tag{4}$$

3. Sealing simulation framework

To perform a sealing lay down simulation, the described flow solver is used with the VOF method to handle the multi-phase flow and the Carreu fluid model to characterize the rheology of the material. The required input is a triangulation of the target geometry, the robot motion of the sealing nozzle and a shear sweep rheometer test of the sealing material.

Due to the high Stoke's number the flow pattern of the sealing material between the nozzle and impact is independent on the flow direction and velocity of the surrounding air. Furthermore, the short application distance implies that gravity has little or no effect on the flow pattern in the air. But, when the material strikes the target's surface it begins to flow and the resulting deposition is highly dependent on the impact angle, material rheology, volymetric flow and the target's geometry. Therefore, in the air the flow dependent sealing spray pattern is reconstructed from experiments and the fluid flow solver simulates the multi-phase surface flow.

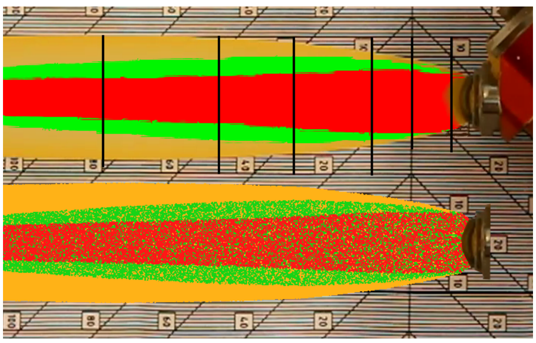

Figure 2: Top: Picture of the static spray pattern for three different volumetric flows (Red $10\,ml/s$, green $15\,ml/s$ and orange $20\,ml/s$). Bottom: Simulated/reconstructed flow pattern for the different volumetric flows visualized with virtual droplets.

The experimental spray pattern and the corresponding reconstruction for three different volumetric flows are shown in Fig. 2.

The reconstruction is based on ray tracing. The width of the spray pattern depends on both volumetric flow and distance from the applicator, and is interpolated from the experimental data. With the help of the ray tracing the impact zone is determined and the volymetric flow, angle and distance dependent impact pattern is predicted with high accuracy. The similar for approach is also implemented for the hollow cone nozzle, but is not presented in this paper.

At the fluid cells corresponding to the impact positions close to the target, the material is inserted as a volumetric material source in the fluid solver and the velocity is set by immersed boundary conditions in the momentum equations. To ensure the no-slip boundary condition on the surface of the target the hybrid immersed boundary condition is adopted [8]. Furthermore, a reference pressure is set in the active fluid domain.

Table 1: Carreau parameters for the sealing material

Parameter	Value	Unit
Zero-shear-rate viscosity, μ_0	886.23	$Pa \cdot s$
Infinite-shear-rate viscosity, μ_∞	1.3418	$Pa \cdot s$
Relaxation time, λ	2.5510	s
Power index, n	-0.034	-

To determine the rheology of the sealing material used at Volvo Cars in Torslanda, tests are performed in a rotary rheometer with a parallel disc. The shear sweep data is fitted to the Carreau rheology model with a least square method, see Table 1. The resulting rheology model is shown in Fig. 3 together with experimental data. In the same test the material density is measured to $1080\,kg/m^3$.

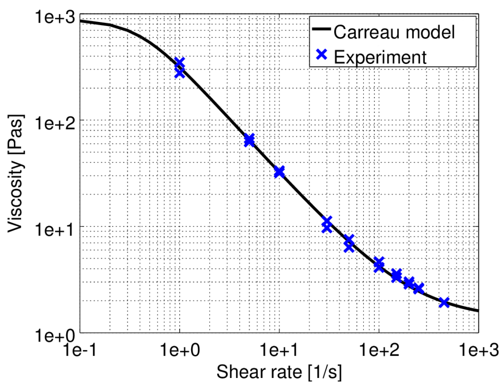

Figure 3: The fitted Carreau model together with rheometer experiments.

Therefore, one time step in the sealing lay down simulations can be summarized as:

1. Update position of applicators and target geometry
2. Calculate the adaptive fluid time step and update grid refinements
3. Connect immersed boundaries with octree grid
4. Update and connect active cells
5. Solve the Navier-Stokes equations (1 - 2)
6. Inject and transport sealing material with the local velocity
7. Interpolate the material volume fraction to the octree nodes
8. Reconstruct the surface of the sealing material on the target by a marching cube algorithm
9. Iterate

4. Results

In this section the sealing lay down simulation is validated for a number of beads on a plate and on a Volvo V40 vehicle. Finally, the importance of resolving the nozzle in the simulation is investigated for a static case.

To validate the simulation results obtained with the IPS Virtual Paint Sealing software, they are compared to measurements for four sealing beads applied to a plate with different process conditions and a production bead on a Volvo V40 vehicle. For the plates the volumetric flow, nozzle to plate distance (TCP distance) and nozzle velocity are stated in Table 2. In Fig. 4 the experimental and simulated beads are shown and in Fig. 5 the average bead widths are compared with excellent agreement.

Table 2: The experimental volumetric flow, nozzle to plate distance (TCP distance) and nozzle velocity for the four validation beads.

Bead number	Volumetric flow	TCP distance	Velocity
–	ml/s	mm	mm/s
1	30	35	400
2	40	35	400
3	50	35	400
4	30	50	400

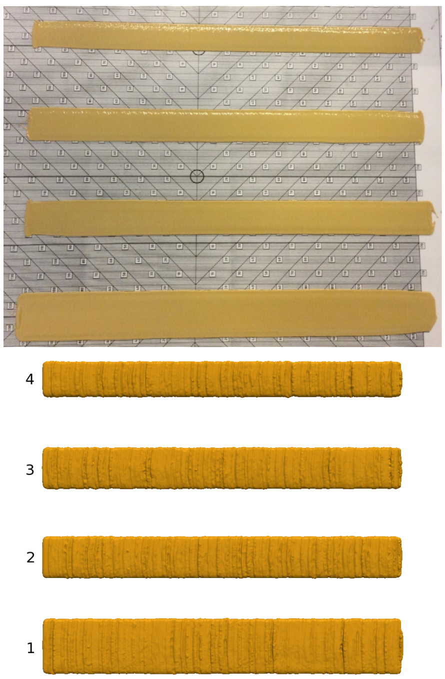

Figure 4: Top: The four experimental beads. Bottom: The corresponding simulated beads.

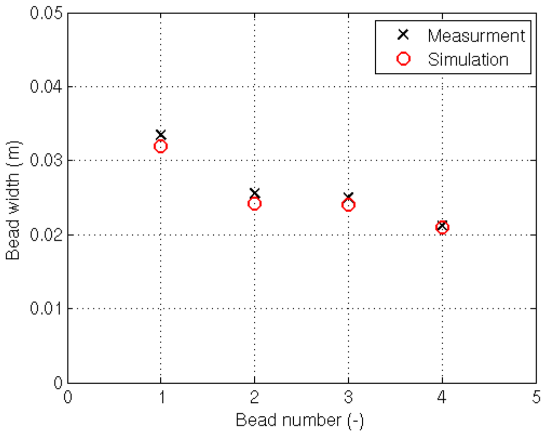

Figure 5: Comparison between the measured and simulated bead widths.

The final verification is performed on a Volvo V40 vehicle produced in the factory in Gent. An interesting bead in production on the internal left fender is chosen. In Fig. 6 the scanned experimental bead (green) is compared with the simulated one (yellow). Notice the good agreement and how the material fills the corners like a ski slope.

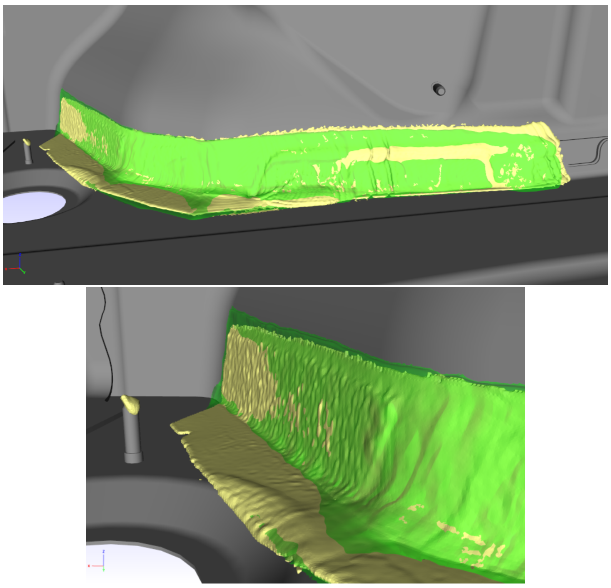

Figure 6: Sealing bead verification on a Volvo V40 vehicle. The scanned experimental bead is shown in transparent green and the simulated bead in yellow.

To validate the projected nozzle simulation where the material is injected close to the target, a static nozzle simulation resolving the material from the injector to the target is performed. The simulation case consists of a flat target and the applicator nozzle is located at $35\,mm$ distance. The spray direction is aligned with the normal direction of the target and the volumetric flow rate of sealing material is $15\,ml/s$. In the projected nozzle simulation the sealing material is injected at the target surface with a corresponding width and velocity of $14.7\,mm$ and $7.38\,m/s$, respectively. A resolved nozzle simulation is also carried out where the flow of sealing material is simulated from the applicator nozzle and through the air to its impact and flow on the target surface. In Fig. 7 a resolved simulation is shown. Both simulations have the same resolution of the respective dynamically refined octree grids, where the smallest cubic cell side is $0.25\,mm$.

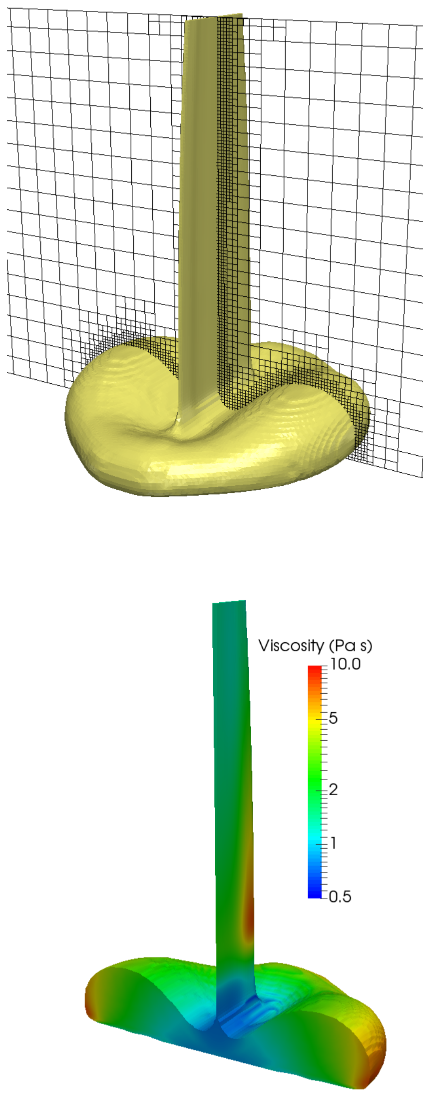

Figure 7: A resolved nozzle simulation, where the flow of the sealing material is simulated in the air and on the target. Top: The sealing material is shown together with the adaptive octree grid. Bottom: The clipped sealing material is colored by the apparent viscosity in log scale.

In Fig. 8 the sealing mass resulting from the projected nozzle simulation is shown at four different simulation times. The corresponding results from the resolved nozzle simulation may be seen in Fig. 9. A slight difference in shape between the two simulations exist. Mainly the difference is that in the resolved simulation a larger part of the sealing material flows and builds up in the perpendicular direction to the flat bead as it hits the target. The same effect is not as significant in the projected nozzle simulation. A slight difference between the results is reasonable, as in the projected nozzle simulation the material is injected with uniform velocity aligned with the normal direction of the target surface, and in the resolved simulation the resulting velocity profile is not uniform. Hence, the local shear rate differs at the impact position and therefore also the resulting viscosity. Because, the physics of the surface flow is dictated by the apparent viscosity the small deviations between the simulations are understood and reasonable.

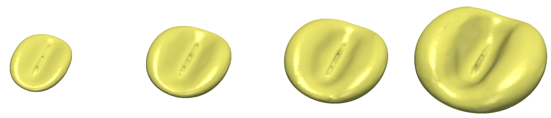

Figure 8: Sealing material from the projected nozzle simulation. From left to right 0.6s, 0.10s, 0.20s and 0.40s.

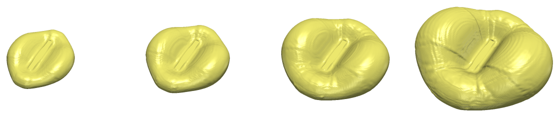

Figure 9: Sealing material for the resolved nozzle simulation. From left to right 0.6s, 0.10s, 0.20s and 0.40s.

A more quantitative comparison of the sealing material from the two simulations is performed by comparing their width and thickness. The width in two directions are compared, namely in the cross direction and the perpendicular direction with regards to the orientation of the flat bead. The two orthogonal directions are clarified in Fig. 10.

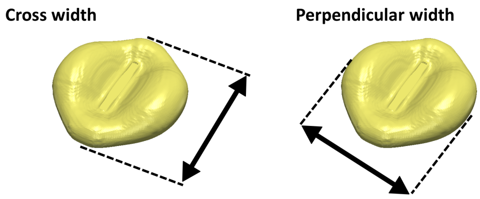

Figure 10: The two directions in which the width of the resulting sealing masses are measured in the flat plate case.

The cross width, the perpendicular width and the thickness of the sealing material produced by the two simulations are plotted against time in Fig. 11 to Fig. 13. The results are consistent with the observation of similar sizes and similar growth pattern is found for both simulations with regards to the three measures. The cross width, shown in Fig. 11, is larger in the projected than in the resolved nozzle simulation. The result is reasonable since more material flows in the perpendicular direction, as discussed above. The perpendicular width, shown in Fig. 12, is very similar for the simulations for the larger part of the simulation time. A slightly smaller width is observed for the projected nozzle simulation for the latter part of simulation, which again is consistent with the previous observations. Also the thickness in the two simulations show very similar patterns, except it being slightly larger in the projected nozzle simulation. The observations clearly demonstrate that the projected nozzle simulation is capable of producing results that to a good approximation predicts the outcome of the resolved nozzle simulation. The average differences between the simulations are 6.7% for the cross width, 1.9% for the perpendicular width and 8.7% for the thickness. From the relative small deviations, it is concluded that the most of the physics are modeled and simulated by reconstructing the sealing material in the air and simulating the impact and surface flow. Further, the projected nozzle simulation reduces the computational cost by orders of magnitude.

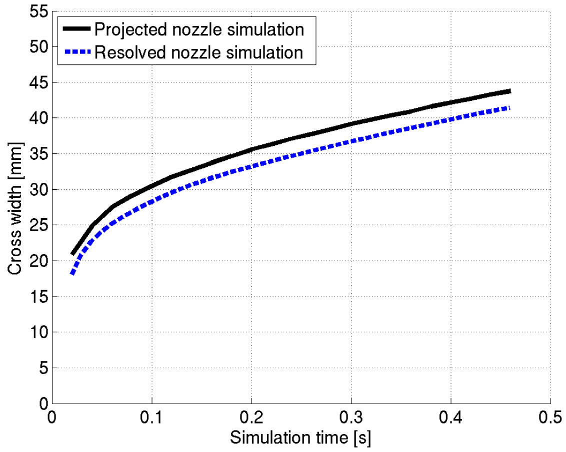

Figure 11: Cross width resulting from the projected and resolved nozzle simulation.

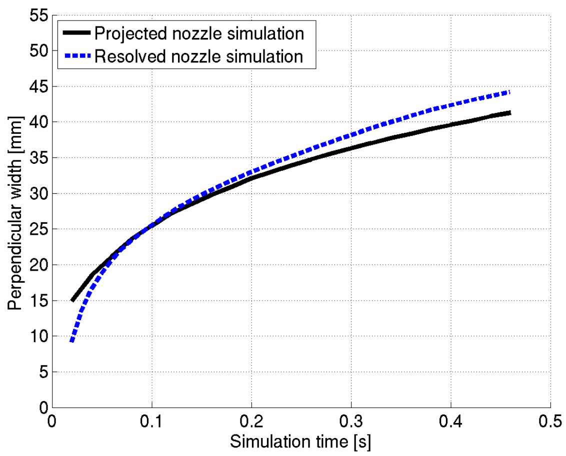

Figure 12: Perpendicular width resulting from the projected and resolved nozzle simulation.

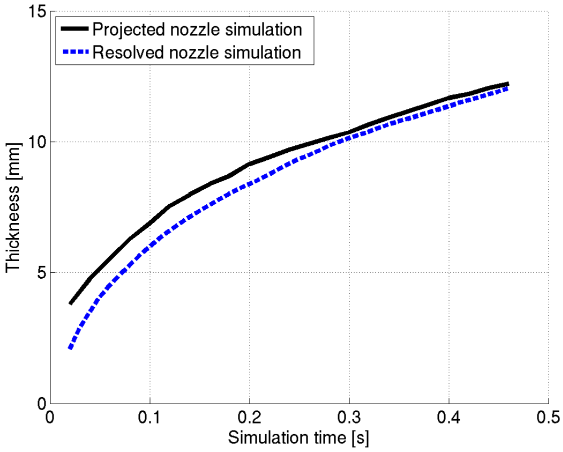

Figure 13: Thickness resulting from the projected and resolved nozzle simulation.

5. Conclusions

From the plate and vehicle validation we conclude that the proposed framework is able to simulate the application of flat bead sealing spray in a reliable way. The projected and the resolved nozzle simulation generate similar results, verifying that the projected nozzle simulation is sufficient to achieve good accuracy. Furthermore, the efficient implementation makes it possible to simulate application of one meter of sealing material in less than an hour on a standard computer. This fact makes it possible to include such detailed simulations in the production preparation process and on-line programming of the sealing robots. This work on virtual sealing is therefore an important step towards the virtual paint factory and contributes to sustainable production by providing simulation tools that can be used by the automotive industry to reduce the time required for introduction of new car models, reduce the cycle-time, reduce the environmental impact and increase quality.

6. Acknowledgments

This work was supported in part by the Sustainable Production Initiative and the Production Area of Advance at Chalmers. The support is gratefully acknowledged. The test geometries and experimental data were provided by Volvo Car Corporation.

References

[1] Industrial Path Solutions (IPS), <http://www.industrialpathsolutions.com>.

[2] IPS IBOFlow, <http://www.ipsiboflow.com>.

[3] Balasubramanian, K.R., Suthakar, T. and Sankaranarayanasamy, K.: Finite element analysis of heat distribution in laser beam welding of AISI 304 stainless steel sheet, Int. J. Manufacturing Research, Vol. 7, No. 1, pp.42–58 (2012)

[4] Bird, R.B., Armstrong, R.C., Hassager, O.: Dynamics of polymer liquids. vol. 1. ,2nd ed, Wiley, New Yourk, (1987)

[5] Domnick, J., Schneider, M.: Computer simulation des Nahtabdichtprozesses im Automobilbau mit Hilfe der VOF-Methode von FLUENT, Fluent CFD Konferenz, Darmstadt, Germany (2003)

[6] van Doormaal, J. P., Raithby, G. D.: Enhancements of the SIMPLE Method for Predicting Incompressible Fluid Flows. Numer. Heat Transfer **7**, 147–163 (1984)

[7] Mark, A., van Wachem, B. G. M.: Derivation and validation of a novel implicit second-order accurate immersed boundary method. J. of Comput. Physics **227**, 6660–6680 (2008)

[8] Mark, A., Rundqvist, R., Edelvik, F.: Comparison Between Different Immersed Boundary Conditions for Simulation of Complex Fluid Flows. Fluid Dyn. Mater. Proc. **7**, 241–258 (2011)

[9] Mark, A., Bohlin, R., Segerdahl, D., Edelvik, F., Carlson, J.S.:Optimisation of Robotised Sealing Stations in Paint Shops by Process Simulation and Automatic Path Planning. Int. J. Manufact. Res. **9**, 4–26 (2014)

[10] O'Gloinn, T., Hayes, C., Hanniffy, P. and Vaugh, K. FEA simulation of conformal cooling within injection moulds, Int. J. Manufacturing Research, Vol. 2, No. 2, pp.162–170 (2007)

[11] Rhie, C. M., Chow, W. L.: Numerical study of the turbulent flow past an airfoil with trailing edge separation. AIAA J1 **21**, 1527–1532 (1983)

[12] Rundqvist, R., Mark, A., Edelvik, F., Carlson, J.S.: Modeling and simulation of viscoelastic fluids using Smoothed Particle Hydrodynamics. Fluid Dyn. Mater. Proc. **7**, 259–278 (2011)

[13] Ubbink, O.: Numerical Prediction of Two Fluid Systems with Sharp Interfaces, PhD thesis, Department of Mechanical Engineering, Imperial College of Science, London, UK (1997)